Available online at www.sciencedirect.com
SCIENCE DIRECT
Polymer 46 (2005) 3001–3005
polymer
www.elsevier.com/locate/polymer

Structure and properties of polyacrylonitrile/single wall carbon nanotube composite films

Huina Guo, T.V. Sreekumar, Tao Liu, Marilyn Minus, Satish Kumar*

School of Polymer, Textile and Fiber Engineering, Georgia Institute of Technology, P.O. Box 0295, Atlanta, GA 30332, USA

Received 4 December 2004; received in revised form 5 February 2005; accepted 9 February 2005
Available online 9 March 2005

Abstract

Polyacrylonitrile (PAN)/single wall carbon nanotube (SWNT) composite films have been processed with unique combination of tensile strength (103 MPa), modulus (10.9 GPa), electrical conductivity (1.5×10^4 S/m), dimensional stability (coefficient of thermal expansion 1.7×10^{-6}/°C), low density (1.08 g/cm^3), solvent resistance, and thermal stability. PAN molecular motion above the glass transition temperature (T_g) in the composite film is significantly suppressed, resulting in high PAN/SWNT storage modulus above T_g (40 times the PAN storage modulus). Rope diameter in the SWNT powder was 26 nm, while in 60/40 PAN/SWNT film, the rope diameter was 40 nm. PAN crystallite size from (110) plane in PAN and PAN/SWNT films was 5.3 and 2.9 nm, respectively. This study suggests good interaction between PAN and SWNT.

Keywords: Polyacrylonitrile; Single wall carbon nanotube; Nanotube

1. Introduction

SWNTs possess high intrinsic strength, stiffness, and electrical conductivity [1,2], and are being incorporate in polymers to obtain composites with unique properties. Various matrix systems that have been studied for this purpose include: poly(vinyl alcohol) (PVA) [3–5], poly (methyl methacrylate) [6–9], poly(*m*-phenylenevinylene-*co*-2, 5-dioctoxy *p*-phenylenevinylene) [10], polypropylene [11], epoxy [12,13], poly(3-octylthiophene) [14,15], polyimide [16,17], polycarbonate [18], polystyrene (PS) [19,20], polyaniline [21], polypyrrole [22], alkoxysilane terminated amide acid (ASTAA) [23], PAN [24,25], and poly(*p*-phenylene benzobisoxazole) [26]. Most of these studies have been carried out at nanotube loadings generally below 10 wt%. However, several studies at high nanotube loadings have been reported. For example, exceptionally tough PVA fibers with 60 wt% SWNTs have been processed [27]. Polyelectrolyte film with 50 wt% SWNT resulted in a tensile strength of 220 MPa [28]. Improvements in modulus, strength, and toughness of SWNT films have been reported with PVA or PS infiltration [29]. PAN, a commercially important polymer and carbon precursor [30], is generally processed from solution [31]. Carbonized PAN/SWNT films are good candidates for electrochemical supercapacitor electrodes [32]. Here, we report PAN/SWNT films with unique combination of tensile, electrical, and thermomechanical properties, low density, and solvent resistance.

2. Experimental

Unpurified HiPCO SWNTs (catalytic impurity based on the thermogravemetric analysis was about 30 wt%) obtained from Carbon Nanotechnologies Inc. were used as received. Dimethyl formamide (DMF) and polyacrylonitrile containing 10% methyl acrylate (random copolymer, molecular weight 100,000 g/mol) were purchased from Sigma-Aldrich and were also used as received. Vacuum dried 0.137 g SWNTs were dispersed in 50 ml DMF by a combination of sonication (Cole-Parmer 8891 bath sonicator) and homogenization using a bio-homogenizer (Biospec products Inc. M133/1281-0). To this SWNT/DMF dispersion, 0.2055 g PAN was added and dissolved by stirring. The PAN/SWNT/DMF solution was cast onto a hot

* Corresponding author. Tel.: +1 404 894 7550.
E-mail address: satish.kumar@ptfe.gatech.edu (S. Kumar).

0032-3861/$ - see front matter © 2005 Elsevier Ltd. All rights reserved.
doi:10.1016/j.polymer.2005.02.013

glass substrate (at 60 °C) to form 15–30 μm thick films. The resulting film was washed repeatedly with distilled water and dried under vacuum at 60 °C. Control PAN and SWNT (buckypaper) films were also made using the same process.

RSA III (Rheometrics Scientific) was used to measure the tensile and dynamic mechanical properties. The gauge length, film width, and strain rate for the tensile test was 25.4, 5 mm and 10%/min, respectively. Dynamic mechanical tests were carried out at 1 Hz at 1 °C/min heating rate. Coefficient of thermal expansion (CTE) was determined using a thermo-mechanical analyzer (TA Instruments TMA 2940) at 0.05 MPa pre-stress on 10 mm long and 2 mm wide films during the second heating cycle when heated at 5 °C/min. In plane dc electrical conductivity was measured by four-probe method. SEM imaging was done on gold-coated films using Leo 1530 Scanning Electron Microscope. X-Ray diffraction studies were conducted on Rigaku R-AXIS IV^{++} equipped with an image plate. The nickel filtered Cu K_α radiation (wavelength = 0.15418 nm) was used and data analysis was done using jade software.

3. Results and discussion

The initial modulus of the composite film is four times the modulus of PAN and an order of magnitude higher than that of the SWNT bucky paper, while the tensile strength of the composite is twice the PAN strength, and 13 times the strength of the bucky paper (Table 1). In this work, bucky paper was made from unpurified tubes. By comparison, in the earlier work we reported bucky paper made from purified tubes exhibiting substantially higher strain to failure (~5%) [33]. Bucky paper strain to failure observed in this work is in better agreement with the value reported by Malik et al. [34]. The storage modulus of PAN/SWNT composite in the plateau region above the glass transition temperature is 40 times the PAN modulus at that temperature (Fig. 1). Based on the tan δ peak position, glass transition temperature of the composite film is 103 °C, while that of the control PAN film it is 91 °C. The decrease in the tan δ magnitude suggests suppression of the PAN molecular motion above the glass transition temperature. The thermal expansion of PAN shows the typical polymer behavior, with coefficient of thermal expansion (CTE) value being much higher above T_g than its value below T_g (Fig. 2, Table 2), while the composite film exhibits only one CTE in the entire temperature range. These properties clearly demonstrate the reinforcing effect of PAN in SWNT and vice-versa.

Table 2
Coefficient of thermal expansion of PAN and PAN/SWNT composite films

Sample	CTE (10^{-6}/°C)	
	35–91 °C (T_g)	91 (T_g)–150 °C
PAN	57	108
PAN/SWNT (60/40)	1.7	0.6
SWNT [44]	−1.5	−1.5

The CTE of the two-dimensionally isotropic composite is given by the equation [35]:

$$\alpha_c = \frac{\alpha_{11}+\alpha_{22}}{2} + \frac{(E_{11}-E_{22})(\alpha_{11}-\alpha_{22})}{2[E_{11}+(1+2\nu_{12})E_{22}]} \quad (1)$$

where

$$\alpha_{11} = \frac{\alpha_{NT}E_{NT}V_{NT} + \alpha_m E_m(1-V_{NT})}{E_{11}} \quad (2)$$

$$\alpha_{22} = (1+\nu_{NT})\alpha_{NT}V_{NT} + (1+\nu_m)\alpha_m(1-V_{NT}) - \nu_{12}\alpha_{11} \quad (3)$$

$$\nu_{12} = \nu_{NT}V_{NT} + \nu_m V_m \quad (4)$$

ν_m and ν_{NT} are the Poisson's ratio for the PAN and SWNT and are taken to be 0.07 [36] and 0.17 [37], respectively. V_{NT} is the volume fraction of SWNT in the PAN/SWNT (60/40) film and is equal to 0.38. The axial modulus of the SWNT (E_{NT}) is 640 GPa [1]. α_m and α_{NT} are the CTEs of PAN and SWNT, respectively, and take the values listed in Table 2. E_m is the modulus of the PAN matrix. In a film with a random nanotube orientation in a plane, E_{11} and E_{22} are related to the composite modulus (E_c) by the equations [35]:

$$E_c = \frac{3}{8}E_{11} + \frac{5}{8}E_{22} \quad (5)$$

$$E_{11} = \frac{1+2(l_{NT}/d_{NT})\eta_L V_{NT}}{1-\eta_L V_{NT}}E_m \quad (6)$$

$$E_{22} = \frac{1+2\eta_T V_{NT}}{1-\eta_T V_{NT}}E_m \quad (7)$$

$$\eta_L = \frac{E_{NT}/E_m - 1}{E_{NT}/E_m + 2(l_{NT}/d_{NT})} \quad (8)$$

$$\eta_T = \frac{E_{NT}/E_m - 1}{E_{NT}/E_m + 2} \quad (9)$$

Table 1
Properties of PAN, PAN/SWNT and SWNT composite films

Sample	SWNT (wt%)	Tensile modulus (GPa)	Tensile strength (MPa)	Elongation at break (%)	Density (g/cm^3)
PAN	0	2.7±0.4	57±4	22.3±6.5	1.01
PAN/SWNT (60/40)	40	10.9±0.3	103±18	1.6±0.6	1.08
SWNT bucky paper	100	1.1±0.1	7.6±1.5	0.6±0.1	0.80

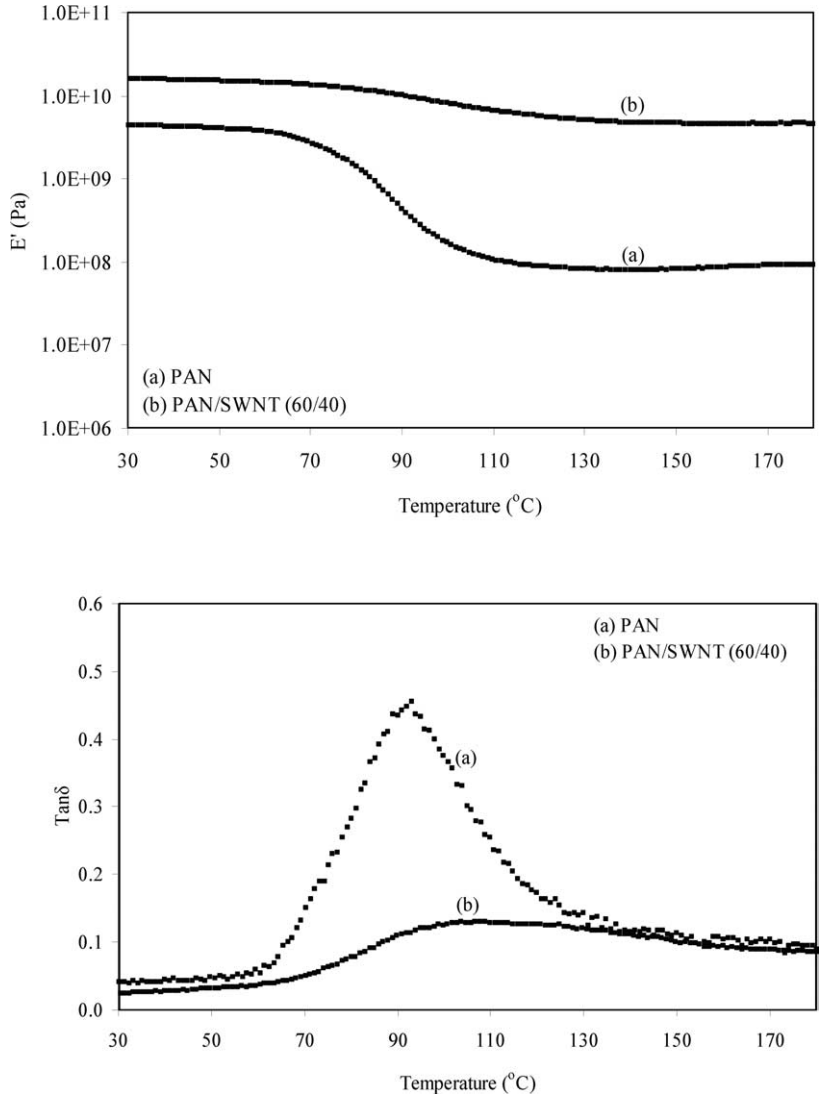

Fig. 1. Storage modulus (E') and tan δ behavior of PAN and PAN/SWNT (60/40) films as a function of temperature.

where l_{NT} and d_{NT} are the length and diameter of nanotube ropes, respectively. Using E_c and E_m values in Table 1, l_{NT}/d_{NT}, E_{11}, E_{22}, were calculated. Using these values in Eqs. (1)–(4), in plane CTE of the composite film was determined to be 1.8×10^{-6}/°C, which is in excellent agreement with the experimental value of 1.7×10^{-6}/ °C.

The electrical conductivity of PAN/SWNT (60/40) composite is 1.5×10^{4} S/m. By comparison, electrically conductivity of PVA/MWNT composite film (40/60) was reported to be 10^{2} S/m^{3}. The conductivity of PAN/SWNT film of the order of 10^{4} S/m is comparable to those of the electrically conducting polymers such as polypyrrole (10^{4} S/m) [38], polythiophene (10^{4} S/m) [39], and polyaniline (10^{3} S/m) [40].

PAN/SWNT composite film retained its shape after being immersed in DMF for three days at room temperature, and only 27% of the PAN in PAN/ SWNT (60/40) composite film dissolved in DMF. From the SEM images (Fig. 3), the rope diameters in the SWNT powder and in the PAN/ SWNT (60/40) films were estimated to be 26 ± 3 nm and 40 ± 2 nm, respectively. In other work, SWNT rope diameters of 30 [41] and 35 nm [32] have been estimated. We attribute these variations in SWNT rope diameter to differences in different batches of nanotubes. Assuming that all PAN is adsorbed on the SWNT rope, the diameter of the PAN wrapped SWNT bundle can be calculated using the following equation:

$$\frac{(d^2+2dR_{SWNT})\rho_{PAN}}{R_{SWNT}^2\rho_{SWNT}}=\frac{m_{PAN}}{m_{SWNT}}$$

where R_{SWNT} is the radius of the SWNT bundle, d is the thickness of PAN coating on SWNT bundle, m_{PAN} and m_{SWNT} are the weight fractions, and ρ_{PAN} and ρ_{SWNT} are the densities of PAN and SWNTs, respectively. The measured density of PAN film (1.01 g/cm^{3}) is lower than the typical

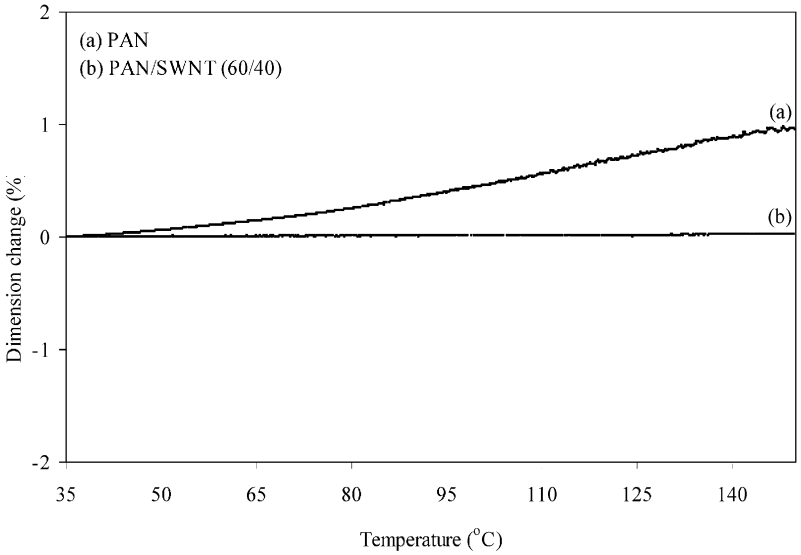

Fig. 2. Thermal expansion of PAN and PAN/SWNT (60/40) films as a function of temperature.

PAN polymer density of 1.18 g/cm^3. During PAN film formation, pore structure forms due to solvent evaporation, resulting in reduced PAN density. Using the measured PAN and SWNT densities (Table 1), and the 26 nm diameter of SWNT bundle, the diameter of the PAN wrapped SWNT bundle is calculated to be 39 nm for the PAN/SWNT (60/40) composite. Using PAN and SWNT theoretical densities of 1.18 and 1.30 g/cm^3, respectively, rope diameter for the composite film was calculated to be 42 nm. Composite rope diameter calculated values of 39 and 42 nm are in excellent agreement with the measured value of ~40 nm (Fig. 3(b)). This suggests that almost all the PAN is adsorbed on the SWNT bundle. The fact that 73% of the total PAN is not accessible to the solvent and cannot be re-dissolved in DMF, further confirms the strong PAN association to SWNT.

PAN and PAN/SWNT films exhibit the characteristic PAN X-ray diffraction peaks at 16.7–16.9, 24.7–26.4 and 28.3–29.6° (Fig. 4) [42]. PAN crystallite size [43] (without instrumental broadening correction) calculated using Scherrer equation from the 110 peak at 16.8° 2θ and PAN X-ray crystallinity [42] values are given in Table 3. The crystal size perpendicular to (110) plane in the composite film is nearly half of the crystal size in the control PAN film. The suppressed motion of the PAN molecule, reduced thermal expansion particularly above the glass transition

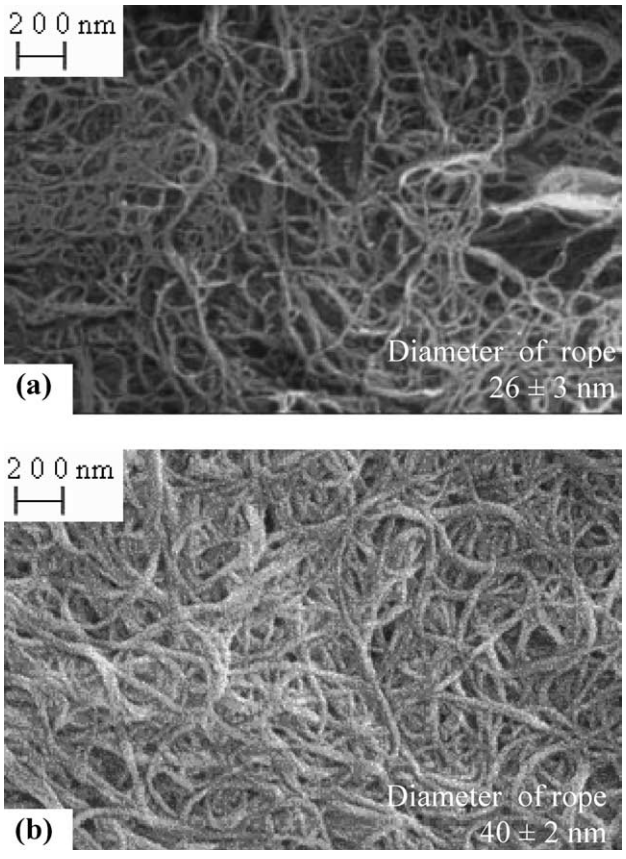

Fig. 3. Scanning electron micrographs of (a) SWNT powder (b) PAN/SWNT (60/40) film.

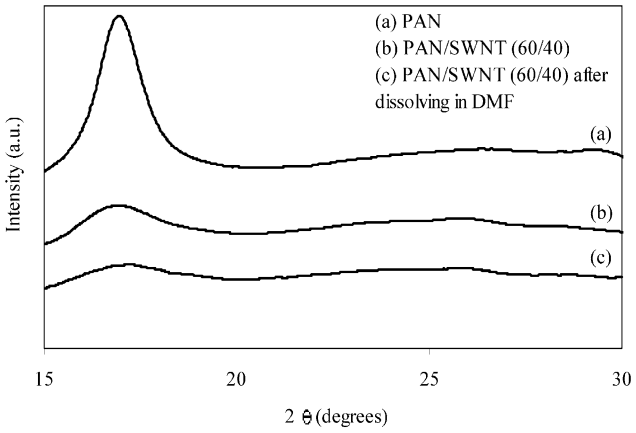

Fig. 4. Wide-angle X-ray diffraction radial scans.

Table 3
WAXD results for the PAN and PAN/SWNT composite films

Sample	Crystal size (nm)	Crystallinity (%)
PAN	5.3	53
PAN/SWNT (60/40)	2.9	45
PAN/SWNT (60/40) after dissolving in DMF	2.6	53

temperature, and decreased PAN solubility in DMF in the composite film, all point to good interaction between PAN and SWNT.

4. Conclusions

SWNTs have been incorporated into PAN to form PAN/SWNT composite films with unique properties. Tensile strength and modulus of the composite films are higher than that of the control PAN or that of the control SWNT bucky paper. The electrical conductivity of the PAN/SWNT composite film in the (60/40) weight ratio is of the order of 10^4 S/m. The PAN/SWNT modulus above glass transition temperature is 40 times the PAN modulus at that temperature. Composite films also show significantly reduced thermal extension at high temperature as compared to PAN film. SEM image of PAN/SWNT film indicates that there is good interaction between PAN and SWNT. Due to PAN adsorption on SWNT, SWNT bundle diameter increased from 26 to 40 nm with 60% PAN. The crystal size in the composite film is significantly smaller than in the control PAN film.

Acknowledgements

Financial support for this work from the Air Force Office of Scientific Research (F49620-03-1-0124), Office of Naval Research (N00014-01-1-0657), and Carbon Nanotechnologies, Inc. is gratefully acknowledged.

References

[1] Baughman RH, Zakhidov AA, Heer WA. Science 2002;297:787.
[2] Thess A, Lee R, Nikolaev P, Dai H, Petit P, Robert J, et al. Science 1996;273:483.
[3] Shaffer MSP, Windle AH. Adv Mater 1999;11:937.
[4] Zhang X, Liu T, Sreekumar TV, Kumar S, Moore VC, Hauge RH, et al. Nano Lett 2003;3:1285.
[5] Zhang X, Liu T, Sreekumar TV, Kumar S, Hu X, Smith K. Polymer 2004;45:8801.
[6] Stéphan C, Nguyen TP, Chapelle ML, Lefrant S, Journet C, Bernier P. Synth Met 2000;108:139.
[7] Haggenmueller R, Gommans HH, Rinzler AG, Fischer JE, Winey KI. Chem Phys Lett 2000;330:219.
[8] Cooper CA, Ravich D, Lips D, Mayer J, Wagner HF. Compos Sci Technol 2002;62:1105.
[9] Benoit JM, Corraze B, Chauvet O. Phys Rev B 2002;65:241405.
[10] McCarthy B, Coleman JN, Czerw R, Dalton AB, Byrne HJ, Tekleab D, et al. Nanotechnology 2001;12:187.
[11] Bhattacharyya AR, Sreekumar TV, Liu T, Kumar S, Ericson LM, Hauge RH, et al. Polymer 2003;44:2373.
[12] Bieruk MJ, Liaguno MC, Radosavljevic M, Hyun JK, Johnson AT. Appl Phys Lett 2002;80:2767.
[13] Kim B, Lee J, Yu I. J Appl Phys 2003;94:6724.
[14] Alexandrou I, Kymakis E, Amaratunga GAJ. Appl Phys Lett 2002;80: 1435.
[15] Kymakis E, Alexandou I, Amaratunga GAJ. Synth Met 2002;127:59.
[16] Chen YC, Raravikar NR, Schadler LS, Ajayan PM, Zhao YP, Lu TM, et al. Appl Phys Lett 2002;81:975.
[17] Lillehei PT, Park C, Rouse JH, Siochi EJ. Nano Lett 2002;2:827.
[18] Sennett M, Welsh E, Wright JB, Li W, Wen JG, Ren Z. Appl Phys A 2003;76:111.
[19] Ramasubramaniam R, Chen J, Liu H. Appl Phys Lett 2003;83:2928.
[20] Pham JQ, Mitchell CA, Bahr JI, Tour JM, Krishanamoorti R, Green 1 PF. J Polym Sci: Part B: Polym Phys 2003;41:3339.
[21] Tahhan M, Truong V, Spinks GM, Wallace G. Smart Mater Struct 2003;12:626.
[22] Anglada NF, Kaempgen M, Skakalova V, Weglikowska UD, Roth S. Diamond Relat Mater 2004;13:2564.
[23] Smith JG, Connell JW, Delozier DM, Lillehei PT, Watson KA, Lin Y, et al. Polymer 2004;45:825.
[24] Sreekumar TV, Liu T, Min BG, Guo H, Kumar S, Hauge RH, et al. Adv Mater 2004;16:58.
[25] Kim SH, Min BG, Lee SC, Park SB, Lee TD, Park M, et al. Fibers Polym 2004;15:198.
[26] Kumar S, Dang TD, Arnold FE, Bhattacharyya AR, Min BG, Zhang X, et al. Macromolecules 2002;35:9039.
[27] Dalton AV, Collin S, Razal J, Munoz E, Ebron VH, Kim BG, et al. J Mater Chem 2004;14:1.
[28] Mamedov AA, Kotov NA, Prato M, Guldi DM, Wicksted JP, Hirsch A. Nat Mater 2002;1:190.
[29] Coleman JN, Blau WJ, Dalton AB, Muñoz E, Collins S, Kim BG, et al. Appl Phys Lett 2003;82:1682.
[30] Donnet JB, Wang TK, Peng JCM, Ribouillat S. Carbon fibers. 3rd ed. New York: Marcel Dekker; 1998.
[31] Masson JC. Acrylic fiber technology and application. New York: Marcel Dekker; 1995.
[32] Liu T, Sreekumar TV, Kumar S, Hauge RH, Smalley RE. Carbon 2003;41:2440.
[33] Zhang X, Sreekumar TV, Liu T, Kumar S. J Phys Chem B 2004;108: 16435.
[34] Malik S, Rösner H, Hennrich F, Böttcher A, Kappes MM, Beck T, et al. Phys Chem Chem Phys 2004;6:3540.
[35] Mallick PK. Composites engineering handbook. New York: Marcel Dekker; 1997. p. 900–5.
[36] Ozkul MH, Mark JE, Aubert JH. J Appl Polym Sci 1993;48:767.
[37] Pipes RB, Hubert P. Comp Sci Tech 2003;63:1571.
[38] Song MK, Kim YT, Kim BS, Kim J, Char K, Rhee HW. Synth Met 2004;141:315.
[39] Patil AO, Heeger AJ, Wudl F. Chem Rev 1988;88:183.
[40] Stejskal J, Hlavatá D, Holler P, Trchová M, Proke J, Sapurina I. Polym Int 2004;53:294.
[41] Uchida T, Kumar S, J Appl Polym Sci, In press.
[42] Gupta AK, Singhal RP. J Polym Sci 1983;21:2243.
[43] Cullity BD. Elements of X-ray diffraction. Reading, MA: Addison-Wesley Publishing Company; 1978. p. 102.
[44] Maniwa Y, Fujiwara R, Kira H, Tou H, Kataura H, Suzuki S, et al. Phys Rev B 2001;64:241402.